ChemComm

A Supramolecular Sensor Array for Selective Immunoglobulin Deficiency Analysis

Journal:	*ChemComm*
Manuscript ID	CC-COM-08-2019-006064.R1
Article Type:	Communication

COMMUNICATION

A Supramolecular Sensor Array for Selective Immunoglobulin Deficiency Analysis

Received 00th January 20xx,
Accepted 00th January 20xx

DOI: 10.1039/x0xx00000x

Yang Liu,[a] Adam D. Gill,[c] Yaokai Duan,[b] Lizeth Perez,[b] Richard J. Hooley*[b,c] and Wenwan Zhong*[a,b]

A host-guest based fluorescence sensor array can sense small differences in protein structure. The combination of three cavitand hosts and two fluorophores to form a 4-component array is sufficient to fully discriminate five structurally similar Ig protein isotypes. The array can be applied to recognize Ig deficiencies in serum, when combined with a Protein L-based extraction process, allowing analysis of immunodeficiency in a simpler, lower cost manner than tests that require multiple specific antibodies.

Detection of protein biomarkers is commonly performed with highly selective antibody-based probes which have diverse applications in clinical practices and therapeutic development. [1] However, each target requires its own selective probe, which is time consuming and costly, and differentiation between protein homologs remains challenging.[2] An alternative and simpler strategy is to use "chemical nose" sensing, which employs arrayed hosts as the recognition elements.[3] This relies on different interactions between the targets and multiple molecular recognition elements to generate signaling patterns that can be easily distinguished by statistical tools. The benefits include simplicity and low cost, as well as the *pan*-selectivity of synthetic receptors that can be adapted to different targets with strategic tuning.[3] Diverse recognition elements such as synthetic receptors, [3c,3d] fluorescent proteins[4] and nanoparticles[5] have been explored, and have allowed detection of a wide range of analytes, including volatile organic compounds, [6] environmental contaminants, [7] peptide modifications, [8] and even cell phenotypes. [9]

Still, a major challenge in chemical nose array sensing is to distinguish analytes with complex secondary and tertiary structures, like protein isotypes. Arrayed sensors that have been previously applied to differentiate proteins use large recognition units that can exploit multivalency in recognition. [10] Even then, the protein targets are restricted to those that have large differences in molecular weight (M_w), isoelectric point (pI), and surface features. For example, arrays using fluorescent or colorimetric nanoparticles (NPs) mainly rely on the charged surface ligands on the NPs forming electrostatic, H-bonding, π-π stacking, or hydrophobic interactions with the protein surface. [11] Peptide chains have also been employed to interact with the core analyte-binding unit, allowing differential binding. [12] However, lack of specificity in target recognition limits the applicability of these arrays towards differentiating protein isotypes. There are some elegant examples that integrate specific protein binders with the spectrally overlapping solvatochromic dyes and FRET pairs to discriminate protein isotypes, but these require multistep synthesis of suitable fluorophore-receptor conjugates. [13]

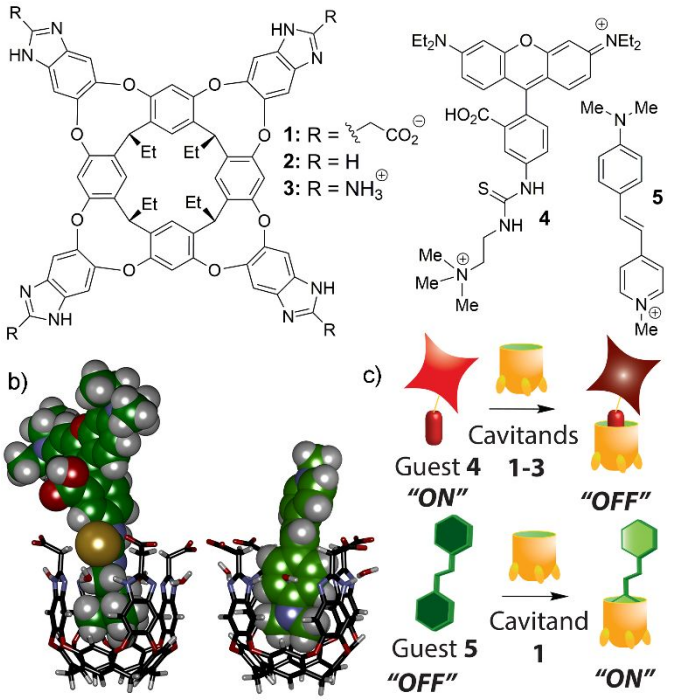

Fig. 1. a) Structure of hosts **1-3**, guests **4** and **5**; b) minimized models of the **1•4** and **1•5** host:guest complexes (SPARTAN); c) Illustration of the turn-on and turn-off fluorescence detection processes.

[a] *University of California - Riverside, Environmental Toxicology Program, Riverside, CA, 92521, U.S.A. E-mail: wenwan.zhong@ucr.edu;*
[b] *University of California - Riverside, Department of Chemistry, Riverside, CA, 92521, U.S.A. E-mail: richard.hooley@ucr.edu.*
[c] *University of California - Riverside, Department of Biochemistry and Molecular Biology, Riverside, CA, 92521, U.S.A.*

Electronic Supplementary Information (ESI) available: experimental procedures and fluorescence data. See DOI: 10.1039/x0xx00000x

Here, we show a cavitand-based sensor that is capable of differential sensing of protein isotypes and apply it to analyze immunoglobulin Ig deficiency. Ig proteins are homologous Y-shaped members of the same family that are distinct in their C regions.[14] Five members in the Ig family, IgA, IgG, IgM, IgE and IgD, are present in serum and can provide key information on patient's immune status.[15] The reference intervals of the three most abundant Ig proteins for healthy adults are: IgA 70–400 μg/ml, IgG 700–1600 μg/ml and IgM 40–230 μg/ml;[15] but deficiencies in even one of the isotypes are linked to increased risk for allergies, autoimmune diseases, and tumor development. Levels of all Ig protein subtypes are determined in clinical practice by radial immunodiffusion assays (RID), [16] ELISAs[17] and nephelometric immunoassays. [18] These assays require multiple antibodies, which can suffer from crosstalk due to their high sequence and structural similarity of these proteins.[14] Moreover, it is often necessary to analyze the differential expression profiles of all five Ig proteins simultaneously. An assay that can rapidly recognize the deficiency in one type of Ig protein by screening several Ig members in a cost-effective manner without using antibodies remains attractive.

Recently, we have developed deep cavitand-based sensor arrays that can be used to sense post-translational modifications (PTM) in peptide strands, [19] showing selective discrimination between different types of modifications, modifications at different residues, [20] and even between identical modifications at different positions on the peptide backbone. [21]

We created the sensor array using three cavitands (**1**, **2** and **3**) and two fluorescent guest molecules (**4** and **5**) (Fig. 1). Guest **4**, a Rhodamine B based fluorophore, binds to all three cavitands at pH 3.0 - 9.0, and the binding strongly quenches its fluorescence. In contrast, guest **5** exhibits a large increase in fluorescence upon binding to cavitand **1**, something not observed with hosts **2** or **3**. These cavitand-dye pairs have been proved to be highly sensitive to the changes in the microenvironment around modified amino acids in peptide strands. [21] As Ig proteins are unstable at low pH, we only applied two sets of pH conditions to the array. The full 8-factor array consisted of the host-guest complexes **1·4**, **2·4** or **3·4** at pH 7.4 or 9.0 (10 mM PBS or carbonate buffer, respectively) with [**4**] = 3 μM and that of cavitand **1**, **2** and **3** being 4, 5, and 5 μM, respectively, and **1·5** at pH 7.4 with [**5**] = 1.5 or 40 μM.

This sensing array was initially applied to samples of the three most structurally different isotypes, IgG, IgM, and IgA (which have Mw = 150, 970 and 320 kDa, respectively). The fluorescence profile of the array resulting from mixing each sensor with 150 μM of each the three Ig proteins is shown in Fig. 2a. We can see that the fluorescence of **1·5** and **1·4** (pH 7.4) increased the most, by 2.5-3.5 and 1.5-2.5 fold, respectively. The largest protein, IgM, induced the largest fluorescence change, and the response pattern of each isotype was quite distinct from that of others. Principal component analysis (PCA) (Fig. S-1) and Jackknife analysis (Table S-3) on the fluorescence patterns showed good differentiation among IgA, IgG, IgM and the no-protein control. Studying the loading scores (Table S-2) from this initial PCA determined that the sensors **1·4**, **2·4**, **3·4** and **1·5** (at a ratio of 1:25) at pH 7.4 made the most important contributions to the grouping effect. As such, we applied this minimal array to the differentiation of all 5 Ig proteins, including IgD, and IgE, which are highly structurally similar to IgG and present a far more stringent sensing challenge. Five repeated measurements on IgG, IgM, IgA, IgD, and IgE were conducted with this array, and the emission profile and scores plots from PCA are shown in Figs. 2b,c. The PCA scores plot exhibited excellent discrimination between the individual Ig isotypes, with the repeated analysis of each Ig protein tightly enclosed in the 95% confidence ellipse. Despite IgM, IgD and IgE having highly comparable pI values, hydrophobicity, and tertiary structures, with many regions having conserved amino acid sequences (Table S1), good separation can be obtained with a minimal array, showing the effectiveness of this simple cavitand:guest recognition system. The sensing is both selective and sensitive: the response was quantified and sensor **1•4** gave the lowest detection limit at 0.77 μg/mL, equivalent to about 1,000 fold dilution of the Ig protein levels in the serum of a healthy individual (Fig. S-2).

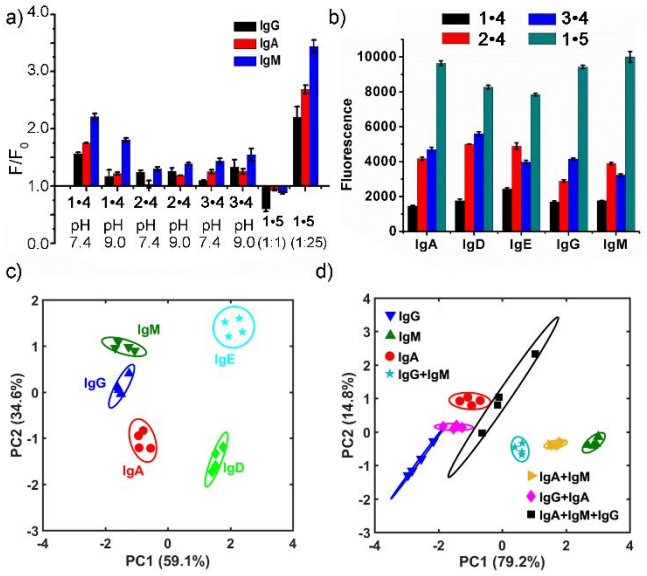

Fig. 2. a) Cavitand:guest response to IgG, IgA and IgM; b) fluorescence data of all five Ig proteins with the minimal **1·4**, **2·4**, **3·4**, **1·5** sensor array; c) PCA plot of five immunoglobulin proteins; d) protein mixtures test with IgA, IgG and IgM. 95% error ellipse was shown surrounding the clusters. [Ig protein] = 150 μg/mL. F_0: sensor fluorescence without protein. Error ellipses were obtained at 95% confidence interval.

We further challenged our array to detect different isotypes in mixtures of proteins. Seven protein mixtures were created, keeping the [total protein] = 150 μg/mL and varying proportions of IgG, IgM, and IgA, and were exposed to the minimal array. The scores plot from PCA on the fluorescence profiles of these protein samples shows good separation in all cases (Fig. 2d, for fluorescence profiles, see Fig. S-3). Interestingly, the two-protein samples (IgA + IgG, IgA + IgM, IgG + IgM) are positioned in-between the single-protein samples containing the two proteins involved. Similarly, the three-protein mixture (IgA + IgG + IgM) resides close to the center of the triangle established by

the three single-protein samples containing only IgG, IgA, or IgM. This shows that the array can differentiate isotypes in Ig protein mixtures, which introduces the possibility of detecting Ig protein depletion in clinical samples collected from patients with immunodeficiencies. We thus tested whether our array could tell apart samples mimicking decreasing concentration in one of the Ig proteins, like IgG. We prepared the mixture of IgA and IgM at an equal mass concentration of 50 μg/mL in 1xPBS, and added varied concentrations of IgG ranging from 0 to 400 μg/mL. The mixture containing no IgG (IgA: IgM: IgG =1:1:0) represents the state of complete IgG depletion, and that with IgA: IgM: IgG being 1:1:8 mimics the healthy range. All samples were significantly distinguishable by the 4-factor array at a confidence level of 95% (Fig. S-4). Most excitingly, the samples mimicking the situations of IgA, IgG, or IgM deficiency can be clearly differentiated from the mixture containing all three Ig proteins at the ratio of IgA: IgM: IgG =1:1:8, i.e. the mimic of "normal" condition, with all four situations well separated from each other (Fig. S-5).

While the array is obviously successful in detecting different protein isotypes, it is challenging to determine why this is so. The initial screening shows that the Ig proteins reverse the quenching effect of the cavitands on guest **4**, and further increase the fluorescence of guest **5**. These responses are not simply due to interaction of the host with the protein, followed by fluorophore displacement: increasing emission of **4** is likely due to displacement and reduced quenching, but guest **5** is turned on upon binding to cavitand **1**, so displacement would reduce the fluorescence. This fluorogenic molecule is sensitive to hydrophobic environments, which suggests an interaction between the cavitand:guest complexes and the Ig proteins.

To gain more information on the mechanism of sensing and the host:Ig binding process, we studied the intrinsic fluorescence originating from tryptophan residues in IgM, which can be quenched if within Förster distance of bound host.[20] The emission spectra of IgA, IgM and IgE upon binding to cavitand **1** at increasing concentration are shown in Fig. S-6. In each case, peak fluorescence at λ = 320-340 nm gradually decreased with increasing [**1**], and the λ_{max} exhibited a significant blue-shift. The blue shift in tryptophan's λ_{max} is evidence for the averaged microenvironment around tryptophan changing from being hydrophilic to hydrophobic, and the fluorescence intensity decrease hints potential quenching of tryptophan fluorescence upon cavitand binding. We also employed limited proteolysis[22] on IgM before and after incubation with cavitand **1** to investigate which amino acid regions on IgM were bound by the host. The peptides cleaved by a 10-min trypsin digestion step (Fig. S-7) were identified by LC-MS/MS and their relative contents were evaluated semi-quantitatively by spectra counting. Incubation with cavitand **1** prevented digestions of the amino acid residues from # 75-125, as well as those between #350 and #400, while enhanced cleavage was observed for those located between #150 and #200 (Fig. S-8). The affected regions are the Fc regions of IgM, which have higher percentage of hydrophobic residues than average of the whole sequence. These results suggest that the lipophilic cavitands likely interact with the Ig protein regions with relatively higher hydrophobicity, causing changes in the fluorescence of bound guests **4** and **5**. We also noticed two tryptophan residues were adjacent to (#148) or included within (#365) these affected regions, partially supporting the tryptophan quenching behaviour observed in Fig. S-6.

While the cavitand array was highly effective in discriminating between Ig isotypes in controlled systems, even being able to detect variations in individual Ig protein concentrations in protein mixtures, the real goal is to analyze Ig proteins in serum. The challenge is that serum contains a variety of other constituents that could interact with the cavitands and prevent detection of the target Ig proteins. To overcome this difficulty, we used magnetic beads conjugated with Protein L to isolate the Ig proteins from the complex serum matrix prior to detection by the cavitand array. Protein L has high affinity to all five Ig proteins (IgG, IgM, IgA, IgE and IgD) through binding to their kappa light chains. Fig. 3 shows the schematic: protein L beads bind to the Ig proteins in serum, then after removal of the beads and elution of the bound Ig proteins, the selective recognition of each individual Ig isoform can be assayed by the cavitand array.

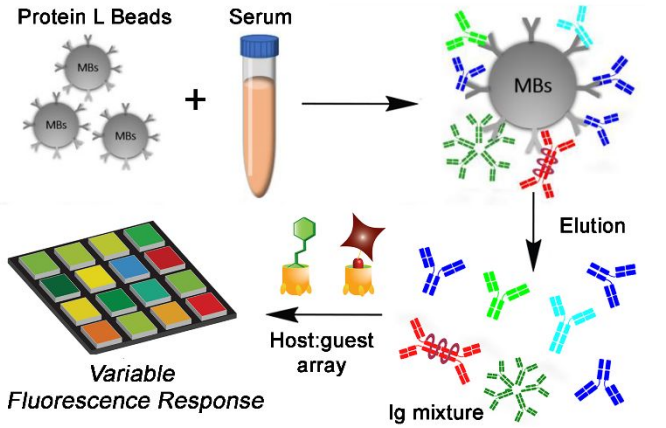

Fig. 3. Scheme of the serum protein immunoglobulin detection. Protein L magnetic beads (MBs) were first mixed with serum, and extracted Immunoglobulins were eluted and measured using the cavitand-guest sensor array.

The commercially available Protein L beads exhibited reasonable recovery for the Ig proteins in serum: with only 0.125 mL of beads, the average extraction efficiency of IgA, IgG, and IgM was about 42%, 60%, and 51%, respectively, in the protein mass range of 3 – 60 μg (Table S-4). Such a protein mass range was selected according to the Ig protein levels found in healthy people with the consideration that only tens of μL of the serum sample would be used for detection of the Ig proteins. On average, 81% of the extracted Ig proteins could be eluted from the beads by the acidic glycine buffer (pH 2) (Table S-5), with the extracted proteins quantified by ELISA.

The Ig protein mixtures representing "normal" concentrations in serum (IgA = 200 μg/mL, IgM = 200 μg/mL and IgG = 1600 μg/mL), or that of IgA, IgG, or IgM deficiency were spiked to a serum sample initially depleted of all Ig proteins. Then the proteins were extracted by the Protein L beads, eluted by glycine buffer, neutralized by sodium hydroxide, and subjected to analysis by our cavitand array. Varied fluorescence

patterns were generated for each sample (Fig. 4a), and PCA resulted in a similar clustering pattern (Fig. 4b) as that obtained from analyzing the same protein mixtures prepared in 1xPBS (Fig. S-5), demonstrating the effectiveness of the Protein L beads in removing all the background molecules while keeping the Ig protein profile intact. For comparison, the Ig protein samples were also analyzed by ELISA. Using three discrete antibodies and three calibration curves (Fig. S-9) allowed the concentration of each Ig protein to be determined (Fig. 4c). Subjecting the chemiluminescence profiles obtained by ELISA to PCA, the four samples were also well differentiated, with a similar grouping pattern and comparable separation distances between different groups (Fig. 4d) to that obtained with our array (Fig. 4b). This result confirms the accuracy of the cavitand-based sensor, and also illustrates its benefits: the arrayed sensor can perform as well as ELISA assays, and does so with simple fluorescence responses instead of the complexity of the ELISA process that requires multiple specific antibodies.

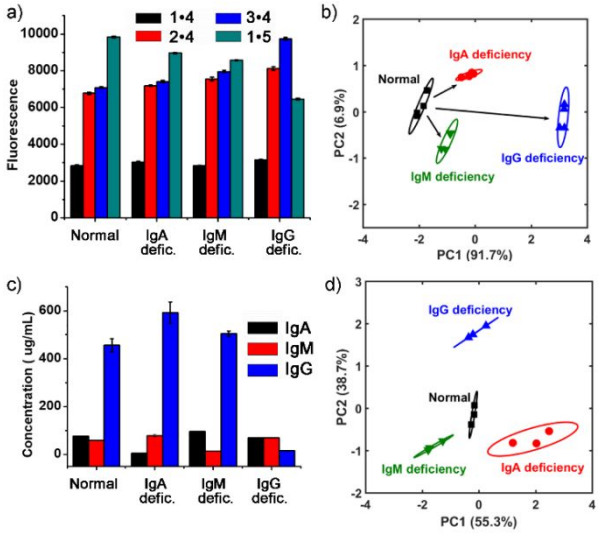

Fig. 4. Spiked serum sample detection using sensor array. Immunoglobulin depleted serum was spiked with different mass ratios of IgA, IgM and IgG. **Normal:** IgA: IgM: IgG = 1:1:8; **IgA deficiency:** IgA: IgM: IgG = 0:1:8; **IgM deficiency:** IgA: IgM: IgG = 1:0:8; **IgG deficiency:** IgA: IgM: IgG = 1:1:0. a) fluorescence response of four serum samples to the 1·4, 2·4, 3·4, 1·5 array; b) PCA scores plot from the fluorescence response; c) ELISA quantification of each immunoglobulin concentration d) PCA scores plot from ELISA results. The error ellipses were obtained at 95% confidence interval.

In conclusion, we have demonstrated the use of an arrayed host:guest indicator system to differentially sense Ig protein isoforms that have high structural similarities. The host molecules are sensitive to hydrophobic regions in proteins, and when mixed with different fluorophores, can discriminate small differences in protein structure. The array is capable of discriminating proteins in controlled media, and can be applied to analyzing Ig deficiencies in serum, when combined with a Protein L-based extraction process. This sensor can assess immunodeficiency in a simpler, and lower cost manner than antibody-based tests.

The authors would like to thank the National Science Foundation (CHE-1707347) for support.

Conflicts of interest

There are no conflicts to declare.

Notes and references

1 N. Rifai, M. A. Gillette, S. A. Carr, *Nat. Biotechnol.* 2006, **24**, 971.
2 a) K. Yamamoto, M. Shiroo, S. Migita, *Science* 1986, **232**, 227; b) L. M. Smith, N. L. Kelleher, *Nat. Methods* 2013, **10**, 186.
3 a) J. R. Askim, M. Mahmoudi, K. S. Suslick, *Chem. Soc. Rev.* 2013, **42**, 8649; b) Y. Geng, W. J. Peveler, V. M. Rotello, *Angew. Chem.* 2019, **131**, 5244; *Angew. Chem., Int. Ed.* 2019, **58**, 5190; c) A. P. Umali, E. V. Anslyn, *Curr. Opin. Chem. Biol.* 2010, **14**, 685; d) Z. Li, J. R. Askim, K. S. Suslick, *Chem. Rev.* 2019, **119**, 231.
4 M. De, S. Rana, H. Akpinar, O. R. Miranda, R. R. Arvizo, U. H. F. Bunz, V. M. Rotello, *Nat. Chem.* 2009, **1**, 461.
5 U. H. F. Bunz, V. M. Rotello, *Angew. Chem.* 2010, **122**, 3338; *Angew. Chem., Int. Ed.* 2010, **49**, 3268.
6 a) Z. Zhang, D. S. Kim, C.-Y. Lin, H. Zhang, A. D. Lammer, V. M. Lynch, I. Popov, O. S. Miljanić, E. V. Anslyn, J. L. Sessler, *J. Am. Chem. Soc.* 2015, **137**, 7769; b) S. H. Lim, L. Feng, J. W. Kemling, C. J. Musto, K. S. Suslick, *Nat. Chem.* 2009, **1**, 562.
7 Y. Liu, T. Minami, R. Nishiyabu, Z. Wang, P. Anzenbacher, *J. Am. Chem. Soc.* 2013, **135**, 7705.
8 a) Y. Liu, L. Perez, A. D. Gill, M. Mettry, L. Li, Y. Wang, R. J. Hooley, W. Zhong, *J. Am. Chem. Soc.* 2017, **139**, 10964; b) B. C. Peacor, C. M. Ramsay, M. L. Waters, *Chem. Sci.* 2017, **8**, 1422; c) K.D. Daze, F. Hof, *Acc. Chem. Res.* 2013, **46**, 937; d) K.D. Daze, T. Pinter, C.S. Beshara, A. Ibraheem, S.A. Minaker, M.C. Ma, R.J. Courtemanche, R.E. Campbell, F. Hof, *Chem. Sci.* 2012, **3**, 2695.
9 A. Bajaj, O. R. Miranda, I. B. Kim, R. L. Phillips, D. J. Jerry, U. H. F. Bunz, V. M. Rotello, *Proc. Natl. Acad. Sci. USA* 2009, **106**, 10912
10 A. T. Wright, M. J. Griffin, Z. Zhong, S. C. McCleskey, E. V. Anslyn, J. T. McDevitt, *Angew. Chem.* 2005, **117**, 6533; *Angew. Chem., Int. Ed.* 2005, **44**, 6375.
11 H. Kong, Y. Lu, H. Wang, F. Wen, S. Zhang, X. Zhang, *Anal. Chem.* 2012, **84**, 4258.
12 a) D. Zamora-Olivares, T. S. Kaoud, K. N. Dalby, E. V. Anslyn, *J. Am. Chem. Soc.* 2013, **135**, 14814; b) W. R. Algar, M. G. Ancona, A. P. Malanoski, K. Susumu, I. L. Medintz, *ACS Nano* 2012, **6**, 11044.
13 a) Z. Pode, R. Peri-Naor, J. M. Georgeson, T. Ilani, V. Kiss, T. Unger, B. Markus, H. M. Barr, L. Motiei, D. Margulies, *Nat. Nanotech.* 2017, **12**, 1161; b) J. Hatai, L. Motiei, D. Margulies, *J. Am. Chem. Soc.* 2017, **139**, 2136.
14 a) H. W. Schroeder Jr, L. Cavacini, *J. Allergy Clin. Immunol.* 2010, **125**, S41; b) K.-i. Kuma, N. Iwabe, T. Miyata, *Curr. Opin. Struct. Biol.* 1991, **1**, 384.
15 A. Gonzalez-Quintela, R. Alende, F. Gude, J. Campos, J. Rey, L. M. Meijide, C. Fernandez-Merino, C. Vidal, *Clin. Exp. Immunol.* 2008, **151**, 42.
16 M. D. Curry, A. Gustafson, P. Alaupovic, W. J. McConathy, *Clin. Chem.* 1978, **24**, 280.
17 C. Hennig, L. Rink, U. Fagin, W. J. Jabs, H. Kirchner, *J. Immunol. Methods* 2000, **235**, 71.
18 J. R. Delanghe, J. P. Chapelle, S. C. Vanderschueren, *Clin. Chem.* 1990, **36**, 1675.
19 Y. Liu, L. Perez, M. Mettry, C. J. Easley, R. J. Hooley, W. Zhong, *J. Am. Chem. Soc.* 2016, **138**, 10746.
20 Y. Liu, L. Perez, M. Mettry, A. D. Gill, S. R. Byers, C. J. Easley, C. J. Bardeen, W. Zhong, R. J. Hooley, *Chem. Sci.* 2017, **8**, 3960.
21 Y. Liu, J. Lee, L. Perez, A. D. Gill, R. J. Hooley, W. Zhong, *J. Am. Chem. Soc.* 2018, **140**, 13869.
22 Y. Feng, G. De Franceschi, A. Kahraman, M. Soste, A. Melnik, P. J. Boersema, P. P. de Laureto, Y. Nikolaev, A. P. Oliveira, P. Picotti, *Nat. Biotechnol.* 2014, **32**, 1036.

Table of Content Entry

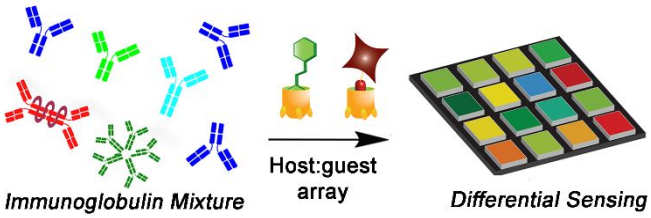

A host-guest based fluorescence sensor array can fully discriminate five structurally similar Ig protein isotypes, and recognize Ig deficiencies in serum.